AGU PUBLICATIONS

JGR

Journal of Geophysical Research: Biogeosciences

RESEARCH ARTICLE
10.1002/2017JG003914

Key Points:
- Nine Earth system models were evaluated for their performance on vegetation carbon density
- ESMs performed well in simulating spatial distribution of carbon densities in root and total vegetation
- Substantial discrepancies were found between modeled and observed root: vegetation ratios and carbon densities

Supporting Information:
- Supporting Information S1
- Data Set S1

Correspondence to:
X. Song and X. Xu,
xsong@mail.sdsu.edu;
xxu@mail.sdsu.edu

Citation:
Song, X., F. M. Hoffman, C. M. Iversen, Y. Yin, J. Kumar, C. Ma, and X. Xu (2017), Significant inconsistency of vegetation carbon density in CMIP5 Earth system models against observational data, *J. Geophys. Res. Biogeosci., 122*, 2282–2297, doi:10.1002/2017JG003914.

Received 23 APR 2017
Accepted 28 JUN 2017
Accepted article online 30 JUN 2017
Published online 9 SEP 2017

Significant inconsistency of vegetation carbon density in CMIP5 Earth system models against observational data

Xia Song[1,2], Forrest M. Hoffman[3], Colleen M. Iversen[3], Yunhe Yin[4], Jitendra Kumar[3], Chun Ma[1], and Xiaofeng Xu[1,2,5]

[1]Biology Department, San Diego State University, San Diego, California, USA, [2]Biology Department, University of Texas at El Paso, El Paso, Texas, USA, [3]Environmental Sciences Division and Climate Change Science Institute, Oak Ridge National Laboratory, Oak Ridge, Tennessee, USA, [4]Institute of Geographic Sciences and Natural Resources Research, Chinese Academy of Sciences, Beijing, China, [5]Northeast Institute of Geography and Agroecology, Chinese Academy of Sciences, Changchun, China

Abstract Earth system models (ESMs) have been widely used for projecting global vegetation carbon dynamics, yet how well ESMs performed for simulating vegetation carbon density remains untested. We compiled observational data of vegetation carbon density from literature and existing data sets to evaluate nine ESMs at site, biome, latitude, and global scales. Three variables—root (including fine and coarse roots), total vegetation carbon density, and the root:total vegetation carbon ratios (R/T ratios), were chosen for ESM evaluation. ESM models performed well in simulating the spatial distribution of carbon densities in root ($r = 0.71$) and total vegetation ($r = 0.62$). However, ESM models had significant biases in simulating absolute carbon densities in root and total vegetation biomass across the majority of land ecosystems, especially in tropical and arctic ecosystems. Particularly, ESMs significantly overestimated carbon density in root (183%) and total vegetation biomass (167%) in climate zones of 10°S–10°N. Substantial discrepancies between modeled and observed R/T ratios were found: the R/T ratios from ESMs were relatively constant, approximately 0.2 across all ecosystems, along latitudinal gradients, and in tropic, temperate, and arctic climatic zones, which was significantly different from the observed large variations in the R/T ratios (0.1–0.8). There were substantial inconsistencies between ESM-derived carbon density in root and total vegetation biomass and the R/T ratio at multiple scales, indicating urgent needs for model improvements on carbon allocation algorithms and more intensive field campaigns targeting carbon density in all key vegetation components.

Plain Language Summary Earth system models (ESMs) have been widely used for projecting global vegetation carbon dynamics, yet how well ESMs performed remains untested. We used observational data to evaluate nine ESMs. ESMs performed well in simulating the spatial distribution of carbon densities in root and total vegetation biomass. However, ESMs performed poorly in simulating absolute carbon densities in root and total vegetation biomass across the majority of land ecosystems, especially in tropical and arctic ecosystems. Particularly, ESMs significantly overestimated carbon density in root and total vegetation biomass in climate zones of 10°S–10°N. Substantial discrepancies between modeled and observed root:total vegetation ratios were found: the root:total vegetation ratios from ESMs were relatively constant, approximately 0.2 across all ecosystems, along latitudinal gradients, and in tropic, temperate, and arctic climatic zones, which was significantly different from the observed large variations in the root:total vegetation ratios (0.1–0.8). The findings in this study indicate an urgent need for model improvements regarding carbon allocation algorithms and more intensive field campaigns targeting carbon density in all key vegetation components.

1. Introduction

Vegetation biomass is one of the most important carbon pools in the biosphere, and it represents the first major pool of carbon entering the ecosystem via photosynthesis [*Chapin et al.*, 2011]. Carbon density in aboveground and belowground vegetation pools is a primary factor controlling carbon sequestration in terrestrial ecosystems [*Jobbagy and Jackson*, 2000; *Mokany et al.*, 2006], and one of the most important factors controlling carbon storage and the carbon residence time in vegetation and soil pools [*Carvalhais et al.*, 2014;

Friend et al., 2014]. However, carbon residence time varies widely among different plant organs [*Raich and Schlesinger*, 1992; *Stephenson and Mantgem*, 2005], from long-lived woody tissue to relatively short-lived deciduous leaves, with fine root falling somewhere in-between. Therefore, the relative amount of carbon in aboveground and belowground vegetation biomass determines ecosystem-level carbon sequestration capacity [*Jackson et al.*, 1996; *Giardina et al.*, 2014; *Canadell et al.*, 1996; *Schenk and Jackson*, 2002]. The root:total (R/T) vegetation biomass ratio has been widely used to quantify vegetation carbon allocation [*Mokany et al.*, 2006]. A large variation of R/T ratios has been reported across biomes [*Mokany et al.*, 2006; *Jackson et al.*, 1996]; for example, tundra, grassland, and cold desert biomes have high R/T ratios, ranging from 0.8 to 0.9, while forests and croplands have relatively low R/T ratios, ranging from 0.1 to 0.3 [*Jackson et al.*, 1996].

Earth system models (ESMs) have been widely used to reconstruct and project climate systems [*Giorgetta et al.*, 2013; *Jungclaus et al.*, 2010], and the past five Intergovernmental Panel on Climate Change (IPCC) reports exclusively depend on ESMs for climate projection. How well the ESMs perform determines the projected behavior of the climate system. In recent decades, the model performance of ESMs has been evaluated against soil organic carbon density and turnover [*Todd-Brown et al.*, 2013; *He et al.*, 2016]. A few studies have also evaluated ESM simulation of vegetation carbon storage at various scales against satellite products [*Anav et al.*, 2013; *Jiang et al.*, 2015; *Friend et al.*, 2014], finding that a large portion of the variability in contemporary global vegetation carbon stocks across ESMs could be explained by differences in vegetation carbon residence time [*Jiang et al.*, 2015]. However, aboveground and belowground vegetation carbon densities simulated by ESMs have not been fully evaluated against observational data.

The large uncertainties in modeled terrestrial carbon processes [*Friedlingstein et al.*, 2006; *Good et al.*, 2013; *Arora et al.*, 2013] have been attributed to a number of mechanisms, including the lack of important soil carbon processes [*Todd-Brown et al.*, 2014; *Xu et al.*, 2013, 2014, 2017], nutrient limitations [*Thornton et al.*, 2009; *Yang et al.*, 2014], and the coarse representation of permafrost dynamics in the arctic [*Schuur et al.*, 2015]. The algorithm responsible for vegetation carbon allocation is another key cause for the ESM uncertainty [*Friedlingstein et al.*, 2006; *Ise et al.*, 2010; *Weng and Luo*, 2011; *De Kauwe et al.*, 2014] due to large differences in carbon residence time for aboveground and belowground vegetation biomass. Thus, it is critically important to accurately evaluate aboveground and belowground vegetation carbon allocation in ESMs in order to better attribute and further reduce the uncertainties in future climate project [*Arora et al.*, 2013; *Hoffman et al.*, 2014]. Further, evaluating the simulated vegetation carbon density has dual implications: (1) the carbon allocation algorithm determines simulated carbon sequestration at the ecosystem level and and (2) projection of climate system dynamics is based on a realistic vegetation carbon density.

Over the past decades, a large number of observational data sets had been compiled for carbon density in different organs, such as root biomass and total vegetation biomass [*Iversen et al.*, 2015; *Gill and Jackson*, 2000; *Mokany et al.*, 2006]. These data sets primarily cover vegetation carbon densities at three different spatial scales: the site level [*Iversen et al.*, 2015; *Mokany et al.*, 2006; *Gill and Jackson*, 2000], biome level (Good Practice Guidance for Land Use, Land-Use Change and Forestry (GPG-LULUCF)) [*IPCC*, 2003], and global level [*Ruesch and Gibbs*, 2008]. These data sets are valuable for evaluating model-simulated vegetation carbon, improving data-model integration, and guiding future field observations [*Peng et al.*, 2015; *Luo et al.*, 2012; *Cadule et al.*, 2010].

The primary goal of this study was to evaluate carbon density in root and total vegetation biomass, as well as the root:total vegetation ratios (R/T ratios) from ESM simulations used in the Coupled Model Intercomparison Project Phase 5 (CMIP5) project. Specifically, three objectives were proposed: (1) to investigate nine ESMs in simulating carbon density in root and total vegetation biomass, as well as the R/T ratios at different spatial scales; (2) to examine model-model differences in terms of simulated root and total vegetation carbon density and analytically attribute the discrepancies to allocation algorithms adopted in these ESMs; and (3) to identify the uncertainty sources that infer urgent needs for model improvements and field observations.

2. Materials and Methods

2.1. Data Sources

Carbon density in root biomass, total vegetation biomass, and the resulting R/T ratios were compiled at three spatial scales: the site level, biome level, and global level (Table 1). The synthesized data sets include

Table 1. Site-, Regional-, and Global-Level Data[a]

Data Set	Description	Data Points	Source
1	Site-level root and total vegetation biomass	276	*Mokany et al.* [2006]
2	Site-level root biomass	258	*Gill and Jackson* [2000]
3	Site-level root and total vegetation biomass	295	*Iversen et al.* [2015]
4	Biome-level root and total vegetation biomass (GPG-LULUCF)	16 biomes	*IPCC* [2003]
5	Global-level root and total vegetation biomass	Spatial map	*Ruesch and Gibbs* [2008]

[a]Notes: GPG-LULUCF: Good Practice Guidance for Land Use, Land-Use Change and Forestry.

829 site-level data points for root and vegetation carbon density [*Mokany et al.*, 2006; *Iversen et al.*, 2015; *Gill and Jackson*, 2000], one data set of biome-level root and total vegetation carbon density [*IPCC*, 2003], and one data set for global-level carbon density in root and total vegetation biomass [*Ruesch and Gibbs*, 2008]. The global distribution of site-level data set of carbon density is illustrated in Figure 1.

2.2. Earth System Models

The CMIP5 ESM simulations of root and total vegetation carbon density were downloaded from the Earth System Grid Federation repository (http://pcmdi9.llnl.gov/esgf-web-fe/) in August 2014. Root carbon density

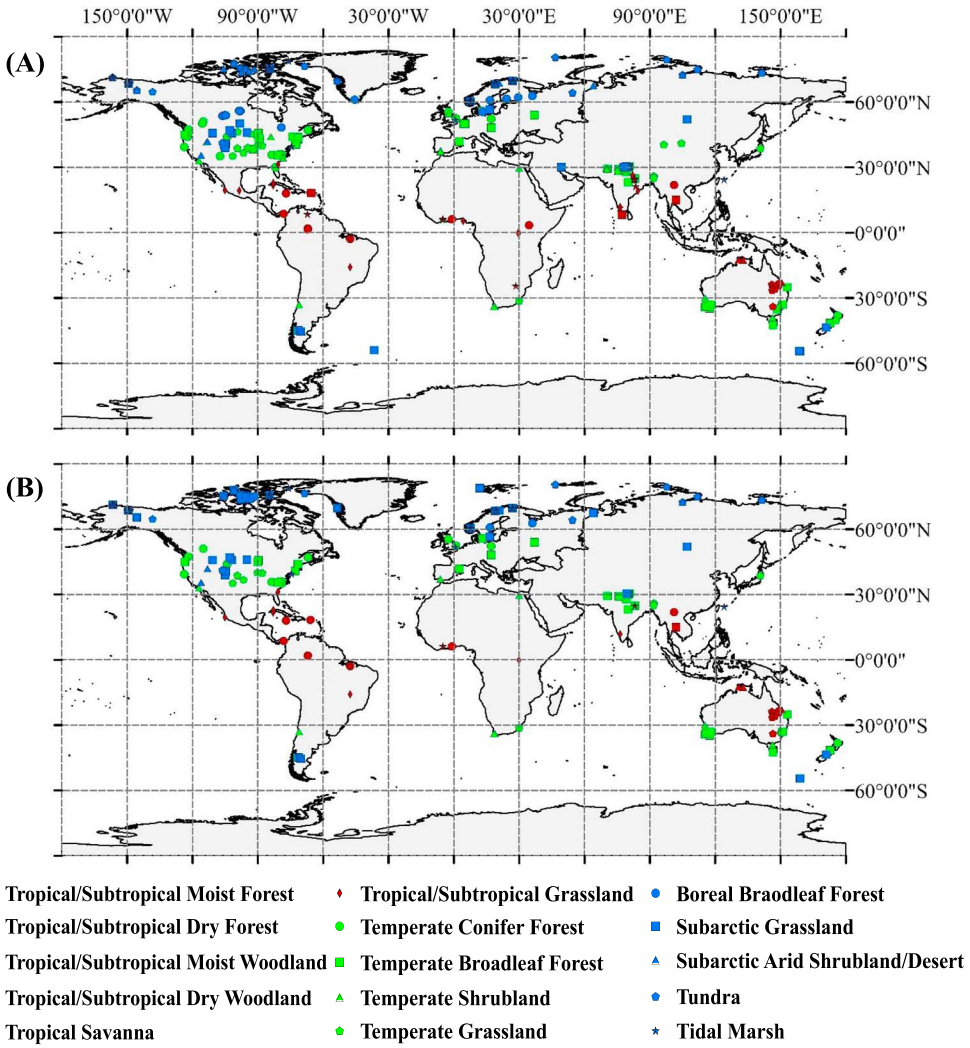

Figure 1. Spatial distribution of site-level data for (a) root and (b) total vegetation biomass carbon.

Table 2. Earth System Models and Their Land Components Used for CMIP5

Models	Source	Land Model	Spatial Resolution
CCSM4 (The Community Climate System Model version 4)	National Center for Atmospheric Research, Unite States	CLM 4.0	0.94° × 1.25°
CESM1-BGC (Community Earth System version 1)	National Center for Atmospheric Research, Unite States	CLM 4.0	0.94° × 1.25°
CESM1-CAM5 (Community Earth System version 1)	National Center for Atmospheric Research, Unite States	CLM 4.0	0.94° × 1.25°
GFDL-ESM2M (Geophysical Fluid Dynamics Laboratory Earth System Model)	Geophysical Fluid Dynamics Laboratory, United States	LM 3.0	2.5° × 2°
IPSL-CM5A-LR (L'Institut Pierre-Simon Laplace Coupled Model version 5A low resolution)	Institute Pierre Simon Laplace, France	ORCHIDEE	3.75° × 1.9°
IPSL-CM5A-MR (L'Institut Pierre-Simon Laplace Coupled Model version 5A medium resolution)	Institut Pierre Simon Laplace, France	ORCHIDEE	3.75° × 1.9°
IPSL-CM5B-LR (L'Institut Pierre-Simon Laplace Coupled Model version 5B)	Institut Pierre Simon Laplace, France	ORCHIDEE	3.75° × 1.9°
NorESM1-ME (Norwegian Earth System Model version 1 (intermediate resolution))	Norwegian Climate Centre, Norway	CLM 4.0	1.9° × 2.5°
NorESM1-M (Norwegian Earth System Model version 1 (intermediate resolution))	Norwegian Climate Centre, Norway	CLM 4.0	1.9° × 2.5°

in the ESM outputs was estimated as the sum of carbon in fine roots and coarse roots, consistent with the compiled observational data. The CMIP5 historical experiments were forced with observed atmospheric composition changes (both anthropogenic and natural sources) and time series of land use and land cover change [*Taylor et al.*, 2011]. The historical runs were long-term experiments, encompassing much of the industrial period (from 1850 to 2005) and sometimes referred to as "twentieth century" simulations. In order to temporally match with the observational data (1990 to 2010), ESM simulation results for 1995–2005 were extracted. It should be noted that this study focused on annual estimates of carbon density in roots and total vegetation biomass; the seasonal variation in vegetation carbon density was not evaluated.

Model outputs from nine ESMs were used in this study, and the primary features of these ESMs are listed in Table 2; detailed information on the land module, vegetation carbon pools, allocation algorithms, and spatial resolution are in Tables S1 and S2 in the supporting information. The nine ESMs evaluated were (1) the Community Climate System Model version 4 (CCSM4), (2) Community Earth System version 1 (CESM1-BGC), (3) Community Earth System version 1-Community Atmosphere Model (CESM1-CAM), (4) Geophysical Fluid Dynamics Laboratory Earth System Model (GFDL-ESM2M), (5) L'Institut Pierre-Simon Laplace Coupled Model version 5A low resolution (IPSL-CM5A-LR), 6) L'Institut Pierre-Simon Laplace Coupled Model version 5A medium resolution (IPSL-CM5A-MR), (7) L'Institut Pierre-Simon Laplace Coupled Model version 5B (IPSL-CM5B-LR), (8) Norwegian Earth System Model version 1 (intermediate resolution) (NorESM1-ME), and (9) Norwegian Earth System Model version 1 (intermediate resolution) (NorESM1-M). NorESM1-M has a horizontal resolution of approximately 2° for the atmosphere and land components and 1° for the ocean and ice components. NorESM1-ME is one version of NorESM that includes prognostic biogeochemical cycling. Three different land models are represented in these ESMs: Community Land Model version 4.0 (CLM4.0) is incorporated in CCSM4, CESM1-BGC, CESM1-CAM, NorESM-ME, and NorESM-M; Land Model 3.0 (LM3.0) is incorporated in GFDL-ESM2M; and Organizing Carbon and Hydrology in Dynamic Ecosystems (ORCHIDEE) is incorporated in IPSL-CM5A-LR, IPSL-CM5A-MR, and IPSL-CM5B-LR. Four model families were identified: the CESM family includes CCSM4, CESM1-BGC, and CESM1-CAM; NorESM family includes NorESM1-M and NorESM1-ME; the GFDL model family includes GFDL-ESM2M; and the IPSL model family includes IPSL-CM5A-LR, IPSL-CM5A-MR, and IPSL-CM5B-LR. Although they share a common land surface model, we treated the CESM-relevant models and NorESM-relevant as two independent families because they are coupled with different ocean and atmosphere model components [*Flato*, 2011]. The reason for choosing these nine ESMs was that these were the only models that produced the required aboveground and belowground carbon density in vegetation components needed for this analysis (see Table S1).

2.3. Definitions of Climate Zones and Biomes

In this study, the data points for root carbon density and total vegetation carbon represented a majority of climatic zones and vegetation types (Figure 1). We grouped the carbon density in roots and total

vegetation into three climatic zones based on their geographic coordinates: (1) tropical/subtropical zone (30°S–30°N), (2) temperate zone (30°S–60°S, 30°N–60°N), and (3) arctic/subarctic zone (60°S–90°S, 60°N–90°N). In addition, 15 vegetation biomes were categorized according to the reported biome types: (1) tropical/subtropical moist forest, (2) tropical/subtropical dry forest, (3) tropical/subtropical moist woodland, (4) tropical/subtropical dry woodland, (5) tropical savanna, (6) tropical/subtropical grassland, (7) temperate coniferous forest, (8) temperate broadleaf forest, (9) temperate shrubland, (10) temperate grassland, (11) boreal broadleaf forest, (12) subarctic grassland, (13) subarctic arid shrubland/desert, (14) tundra, and (15) tidal marshes. In order to evaluate the ESM performance against site-level data, the values of individual grid cells corresponding to the geographic coordinates of observational data were extracted from the model outputs of individual ESMs.

2.4. Data Processing and Statistical Analysis

The R program and NCO (netCDF Operators: http://nco.sourceforge.net/) were used for analyzing the observational data, and processing and visualizing CMIP5 model outputs. An analysis of variance test was carried out within R Program 3.1.1.1 (www.r-project.org). All data points were spatially widely distributed and independent; the original data did not meet normality and were therefore log-transformed before analysis. The mean and 95% confidence boundaries (mean ± 1.96 standard deviation) of carbon density and R/T ratios were then converted back to original values for reporting. If log-transformation was sufficient for a normal distribution, the Wilcoxon signed rank test was used to assess statistical significance for comparisons between observational data and modeled outputs. To be consistent, the underestimation of observed data by model output was reported as negative, while overestimation was positive in the text.

3. Results

3.1. Comparisons of Carbon Density and R/T Ratios Across Climate Zones

3.1.1. Root Carbon Density Across Climate Zones

Modeled root carbon density differed from observed root carbon density, but this depended on the climatic zone. In the arctic zone, the mean of modeled root carbon density was 0.59 (95% confidence interval (CI): 0.51–0.68) kg C/m^2, consistent with the observed root carbon density of 0.57 (95% CI: 0.46–0.70) kg C/m^2 (Figure 2a) ($p = 0.80$). In the temperate zone, the mean of modeled root carbon density was 0.33 (95% CI: 0.29–0.38) kg C/m^2, only ~44% of the observed root carbon of 0.75 (95% CI: 0.65–0.86) kg C/m^2 (Figure 2b) ($p < 0.001$). In the tropical zone, the mean of modeled results was 1.94 (95% CI: 1.53–2.45) kg C/m^2, more than twice the observed root carbon density of 0.68 (95% CI: 0.51–0.91) kg C/m^2. However, separating the tropical climate zone into two subclimate zones gave a more nuanced view of the data-model discrepancies. In the subtropical zones of 10°S–30°S and 10°N–30°N, ESMs significantly underestimated root carbon density by approximately −37% ($p < 0.001$), while in the tropical zone of 10°N–10°S, ESMs significantly overestimated root carbon density by approximately 183% ($p < 0.001$).

3.1.2. Total Vegetation Carbon Density Across Climate Zones

Similarly, modeled total vegetation carbon density differed from the observational data. In the arctic zone, the mean of modeled total vegetation carbon density was 2.76 (95% CI: 2.34–3.25) kg C/m^2, significantly greater than the observed vegetation carbon density of 1.84 (95% CI: 1.40–2.41) kg C/m^2 (Figure 2d) ($p < 0.05$). In the temperate zone, the mean of modeled vegetation carbon density was 1.81 (95% CI: 1.57–2.08) kg C/m^2, approximately 64% of the observed vegetation carbon of 2.84 (95% CI: 2.35–3.44) kg C/m^2 (Figure 2e) ($p < 0.001$). In the tropical zone, the mean of modeled total vegetation carbon density was 11.20 (95% CI: 8.89–14.10) kg C/m^2, much higher than the observed vegetation carbon density of 4.20 (95% CI: 2.87–6.13) kg C/m^2 (Figure 2f) ($p = 0.04$). Similar to root carbon density, ESMs significantly underestimated total vegetation carbon density by approximately −38% in the 10°S–30°S and 10°N–30°N subtropical zones ($p < 0.001$), while significantly overestimating total vegetation carbon density by approximately 167% in the 10°N–10°S tropical zone ($p < 0.001$).

3.1.3. R/T Ratios Across Climate Zones

There were substantial discrepancies between modeled and observed ratios of root carbon to total vegetation carbon (R/T ratios) in the three climate zones (Figures 2g–2i). While there was a wide variation in R/T ratios across the observational data, the modeled R/T ratios were generally static, equal to ~0.2 across all three climate zones. The observed R/T ratios in the tropics, temperate, and arctic zones were 0.21 (95% CI:

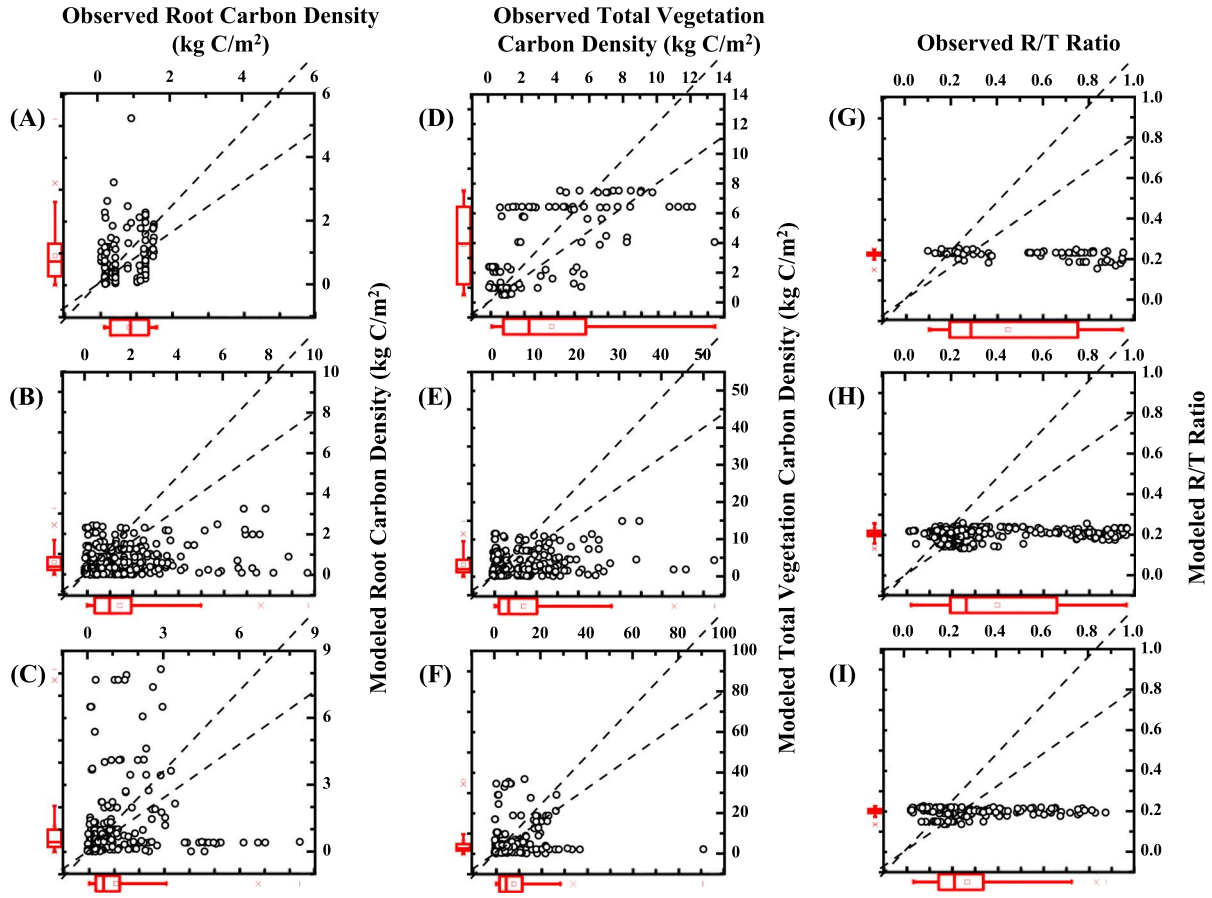

Figure 2. Paired comparisons of carbon density and root:total vegetation carbon ratio in CMIP5 model outputs and observational data sets in three different climate zones (Notes: the box plot means the variation range of root carbon from modeled results and observational data in this climatic zone: (a) root carbon density in arctic, (b) root carbon density in temperate, (c) root carbon density in tropics, (d) total vegetation carbon density in arctic, (e) total vegetation carbon density in temperate, (f) total vegetation carbon density in tropics, (g) R/T ratio in arctic, (h) R/T ratio in temperate, and (i) R/T ratio in tropics).

0.19–0.23), 0.31 (95% CI: 0.28–0.34), and 0.56 (95% CI: 0.51–0.63), respectively. However, ESM simulations of R/T ratios in these climate zones averaged 0.20 (95% CI: 0.19–0.21), 0.20 (95% CI: 0.20–0.21), and 0.22 (95% CI: 0.22–0.23). The underestimations were approximately −6% (p = 0.1), −34% ($p < 0.001$), and −60% ($p < 0.001$) for the tropics, temperate zone, and the arctic zones, respectively.

3.2. Comparisons of Carbon Density and R/T Ratios at Biome Level

3.2.1. Biome-Level Root Carbon Density

The ESMs underestimated root carbon density in 10 biomes out of 15 biomes, including tropical/subtropical moist woodlands (−55%, p = 0.002), tropical/subtropical dry woodlands (−75%, p = 0.001), temperate coniferous forest (−51%, $p < 0.001$), temperate broadleaf forest (−70%, $p < 0.001$), temperate shrublands (−60%, p = 0.03), temperate grasslands (−56%, p = 0.01), and tundra (−68%, p = 0.01); ESMs slightly (but not significantly) underestimated the root carbon density for tropical/subtropical dry forest (−21%, p = 0.69), subarctic grasslands (−26%, p = 0.21), and subarctic arid shrubland/dessert (−17%, p = 0.55). ESMs overestimated root carbon density in five biomes, including tropical/subtropical moist forest (37%, p = 0.01) and tropical savanna (84%, p = 0.04), with smaller overestimations for tropical/subtropical grasslands (17%, p = 0.41) and boreal broadleaf forest (15%, p = 0.07). The overestimation was 94% in tidal marshes. For most biomes, the differences between observed and simulated root carbon in ESMs were larger than 40% (Figure 3a).

3.2.2. Biome-Level Total Vegetation Carbon Density

There were large discrepancies in total vegetation carbon density between ESMs and observational data in all 15 vegetation biomes (Figure 3b). ESMs underestimated total vegetation carbon density for six biomes,

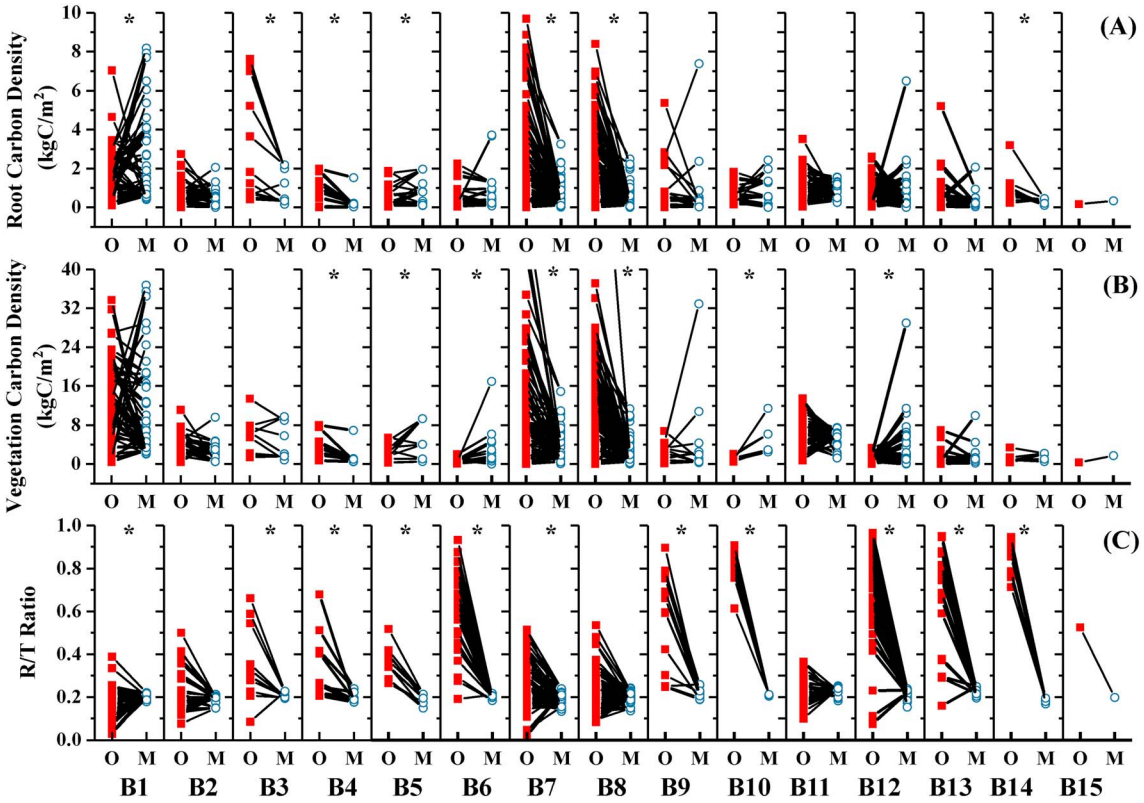

Figure 3. Comparisons of CMIP5 model outputs against observational data sets (The asterisk indicates significant differences between observations (O) and modeled results (M) at $P < 0.05$. A: root carbon density; B: total vegetation carbon density; C: root/total vegetation ratio; B1: tropical/subtropical moist forest; B2: tropical/subtropical dry forest; B3: tropical/subtropical moist woodland; B4: tropical/subtropical dry woodland; B5: tropical savanna; B6: tropical/subtropical grassland; B7: temperate conifer forest; B8: temperate broadleaf forest; B9: temperate shrubland; B10: temperate grassland; B11: boreal broadleaf forest; B12: subarctic grassland; B13: subarctic arid shrubland/desert; B14: tundra; B15: tidal marsh; tropical climate zone includes B1–B6; temperate climate zone includes B7–B10; arctic climate zone includes B11–B14; B15 is not assigned to any climate zone due to its broad distribution; the red solid rectangles represent observational values, while the blue open circles modeled values; each pair of observational and modeled result was connected with a solid black line).

including tropical/subtropical dry woodland (−73%, $p < 0.001$), temperate coniferous forest (−44%, $p < 0.001$), and temperate broadleaf forest (−82%, $p < 0.001$), with smaller (and not statistically significant) underestimations in tropical/subtropical moist forest (−12%, $p = 0.17$), tropical/subtropical dry forest (−20%, $p = 0.34$), and tropical/subtropical moist woodland (−27%, $p = 0.11$). In contrast, ESMs overestimated total vegetation carbon density in nine biomes, including tropical savanna (71%, $p = 0.07$); tropical/subtropical grassland (182%, $p < 0.001$); temperate grasslands (275%, $p < 0.001$); subarctic grasslands (167%, $p < 0.001$); subarctic arid shrubland/desert (108%, $p = 0.006$), with smaller (and not statistically significant) overestimations in temperate shrubland (7%, $p = 0.68$); boreal broadleaf forest (11%, $p = 0.44$); and tundra (32%, $p = 0.41$). The overestimation was 427% in tidal marshes.

3.2.3. Biome-Level R/T Ratios

Two observational data sets were used to evaluate ESM simulations of R/T ratios (Figure 3c); one data set from our literature syntheses and another data set from the IPCC (GPG-LULUCF). The discrepancies between the two observational data sets were less than 32%, and the mean of the two observational data sets was used for evaluating ESM performances. ESMs underestimated R/T ratios in 12 biomes and overestimated R/T ratios in three biomes. ESMs significantly underestimated the R/T ratios for tropical/subtropical moist woodland (−33%, $p = 0.03$), tropical/subtropical dry woodland (−36%, $p < 0.001$), tropical savanna (−47%, $p < 0.001$), tropical/subtropical grassland (−66%, $p < 0.001$), temperate shrubland (−57%, $p < 0.001$), temperate grassland (−74%, $p < 0.001$), subarctic grassland (−70%, $p < 0.001$), subarctic arid shrubland/desert (−63%, $p < 0.001$), and tundra (−78%, $p < 0.001$). The underestimation in R/T ration is 62% for the tidal marshes. ESMs slightly (but not significantly) underestimated R/T ratios for tropical/subtropical dry forest (−6%, $p = 0.55$) and temperate conifer forest (−11%, $p < 0.001$). Meanwhile, ESMs significantly

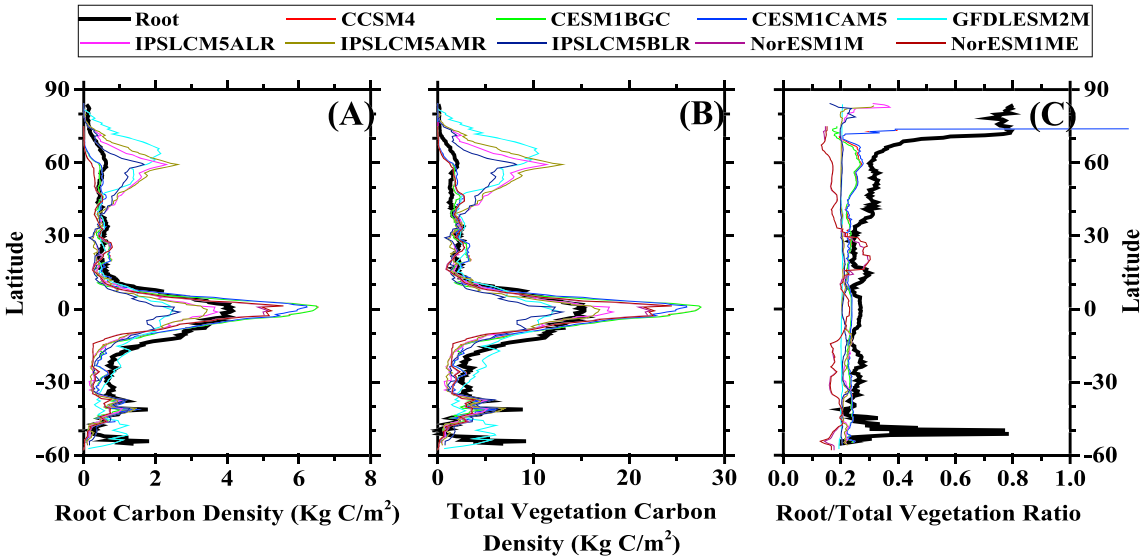

Figure 4. Latitude patterns of (a) root carbon density, (b) total vegetation carbon density, and (c) R/T ratio of CMIP5 models output and observational data.

overestimated R/T ratios for the tropical/subtropical moist forest (53%, $p < 0.001$) and boreal broadleaf forest (10%, $p = 0.006$), and slightly (but not significantly) overestimated the R/T ratios for temperate broadleaf forest (3%, $p = 0.35$).

Both observational data sets showed large variations in the R/T ratio across the 15 biomes (Figure 3c), ranging from 0.13 (tropical forest) to 0.8 (arctic). However, ESMs did not capture this interbiome variation. R/T ratios varied within a fairly narrow range across most ESMs, ranging from 0.20 to 0.31 for CCSM4, 0.18 to 0.31 for CESM1-BGC, 0.19 to 0.33 for CESM1-CAM5, 0.19 to 0.27 for GFDL-ESM2M, 0.19 to 0.28 for IPSL-CM5A-LR, 0.17 to 0.26 for IPSL-CM5A-MR, 0.19 to 0.27 for IPSL-CM5B-LR, 0.09 to 0.17 for NorESM1-M, and 0.09 to 0.17 for NorESM1-ME.

3.3. Latitudinal Comparisons of Carbon Density and R/T Ratios

3.3.1. Latitudinal Comparisons of Root Carbon Density

All nine ESMs performed well in capturing the latitudinal distribution of root carbon density in the Northern Hemisphere, while the simulated latitudinal patterns in the Southern Hemisphere were largely biased (Figure 4a). The ESMs underestimated root carbon density in the latitudinal zones of 70°S–50°S (−80%, $p = 0.006$), 30°S–10°S (−56%, $p < 0.001$), and 50°S–30°S (−27%, $p < 0.001$). In the tropical zone between 10°S and 10°N, a substantial difference was observed among the nine ESMs; for example, GFDL-ESM2M and IPSL-CM5B-LR significantly underestimated (< −50%), while CCSM4, CESM1-BGC, NorESM1-M, and NorESM1-ME significantly overestimated root carbon density (>50%). However, the multiple-model average was relatively consistent with the observational results (<4% difference, $p = 0.001$). In the Northern Hemisphere, ESMs underestimated root carbon density in two latitudinal zones, −62% ($p < 0.001$) for 70°N–90°N and −13% ($p < 0.001$) for 10°N–30°N; ESMs performed quite well in capturing root carbon density for 30°N–50°N. However, four models (GFDL-ESM2M, IPSL-CM5A-LR, IPSL-CM5A-MR, and IPSL-CM5B-LR) significantly overestimated root carbon density in the latitudinal zone of 50°N–60°N (>200%).

3.3.2. Latitudinal Comparisons of Vegetation Carbon Density

Similar to root carbon density, a significant underestimation of total vegetation carbon density occurred in the latitudinal zones of 70°S–50°S (−80%, $p = 0.007$), 30°S–10°S (−49%, $p < 0.001$), and 50°S–30°S (−17%, $p = 0.02$). A significant overestimation occurred in the latitudinal zones of 70°N–90°N (381%, $p < 0.001$), 50°N–70°N (110%, $p < 0.001$), and 30°N–50°N (35%, $p < 0.001$). The ESMs performed quite well on total vegetation carbon density in the latitudinal zone of 10°N–30°N, with less than a 7% ($p = 0.24$) discrepancy. For the latitudinal zone 10°S–10°N, there were again large intermodel discrepancies; CCSM4, CESM1-BGC, NorESM1-M, and NorESM1-ME significantly overestimated total vegetation carbon density; however, the multiple-model average was relatively consistent with observational results (<12% discrepancy, $p = 0.17$).

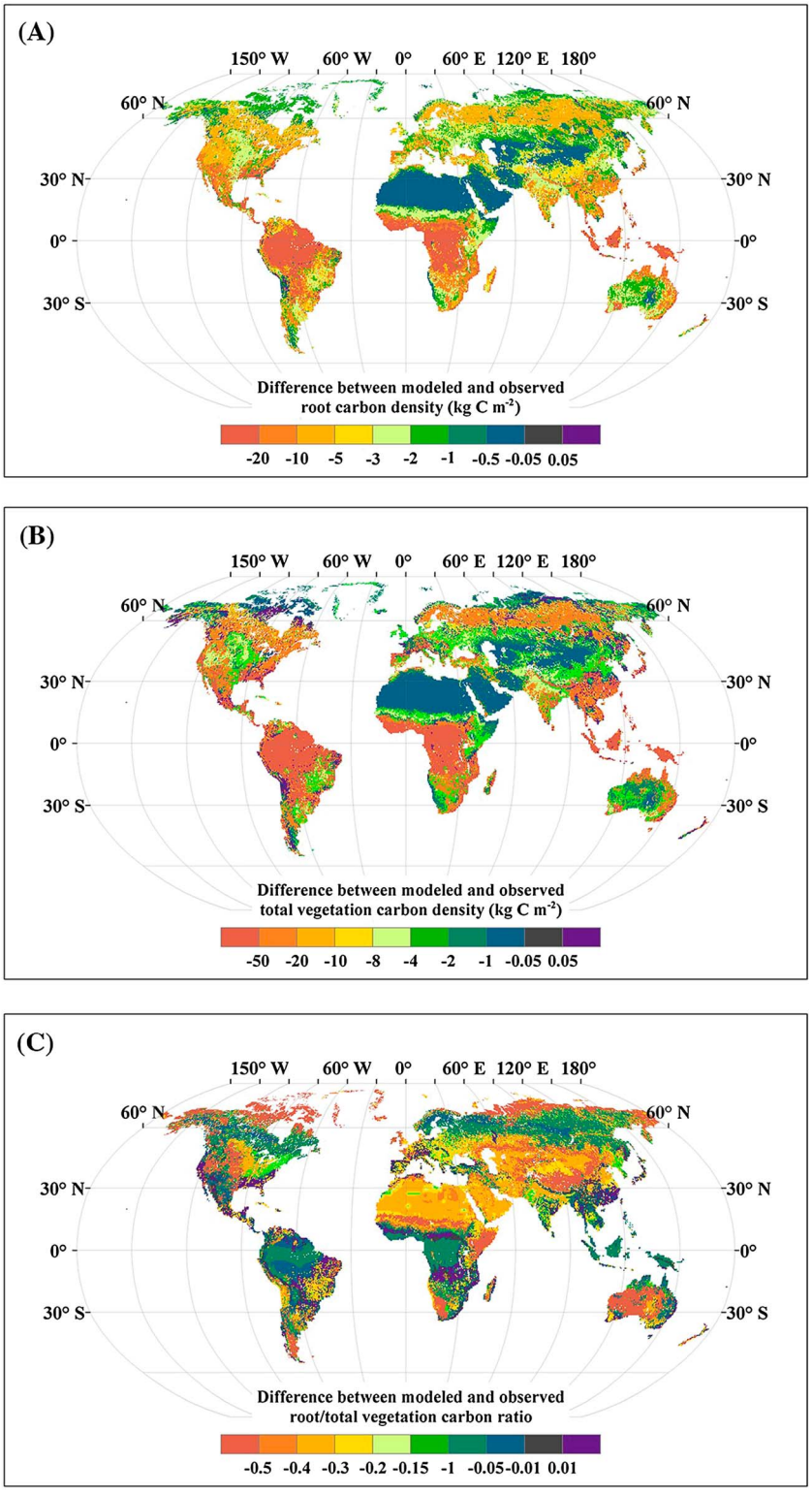

Figure 5. Differences of (a) root carbon density, (b) vegetation carbon density (kg/m^2), and (c) R/T ratios of CMIP5 models mean and observational data (ESMs mean minus observational data; positives indicate overestimation and negatives indicate underestimation).

The latitudinal comparisons of total vegetation carbon density were consistent with results obtained from site-level comparisons. In the tropical and temperate biomes, ESMs underestimated total vegetation carbon density, but in the arctic region ESMs severely overestimated total vegetation carbon density. The most obvious discrepancy occurred between 40°N and 70°N with a substantial overestimation. In addition, discrepancies also occurred in a majority of the Southern Hemisphere and tropical areas (Figures 4a and 4b).

3.3.3. Latitudinal Comparisons of R/T Ratios

There was a large discrepancy between observational and simulated R/T ratios along latitudinal gradients (Figure 4c). ESMs significantly underestimated R/T ratios for most regions and across latitudes ($P < 0.001$). The underestimation could be as large as $< -80\%$ ($p = 0.002$) for high-latitude areas, to $> -10\%$ ($p < 0.001$) for tropical regions. Meanwhile, there were remarkable intermodel variations. For example, NorESM1-M and NorESM1-ME underestimated the R/T ratios by -80% in the climate zone of 70°N–75°N and overestimated R/T ratios by 10% in the climate zone of 20°N–30°N. The CESM family (CCSM4, CESM1-BGC, and CESM1-CAMs) underestimated R/T ratios by -65% for 70°N–75°N and was consistent with observational data for the region of 20°N–30°N (underestimated $> -5\%$).

3.4. Global Consistency Between Modeled and Observational Carbon Density

Across the globe, patterns in modeled and observed carbon density in root and total vegetation carbon density were generally consistent, although the magnitude varied (Figure 5). ESM-simulated patterns in root carbon density were generally consistent with observational data ($r = 0.56$); larger root carbon density occurred in tropical areas and lower root carbon density occurred in arctic and temperate regions. However, an obvious discrepancy was detected for the absolute values of root carbon density (Figure 5a); ESMs substantially underestimated root carbon density in the tropical zone (e.g., Amazonia and African, and Asian tropical forest) and overestimated root carbon density in the temperate and arctic zones (~1 kg C/m^2 difference).

The bias of modeled total vegetation carbon density was highly consistent with root carbon density ($r = 0.96$) (Figure 5b): larger underestimation in Amazonia and African tropical forests and intermediate underestimation for the temperate and arctic regions. For the R/T ratios, large bias existed for the Africa desert and the semiarid region in central Asia. In consistent with analysis across different biomes, no R/T ratio variation was captured in ESMs; the modeled R/T ratios were relatively narrow across biomes. The spatial distribution of the bias (modeled-observed R/T ratio) showed contrasting patterns to those for carbon density in root ($r = -0.16$) and total vegetation carbon ($r = -0.15$). The ESMs performed very well in simulating spatial patterns of the carbon density in root and total vegetation biomass. The spatial distribution of the mean of nine models was in a good agreement with observational data in root ($r = 0.71$) and total vegetation carbon density ($r = 0.62$). However, the carbon partitioning between aboveground and belowground biomass, expressed as R/T ratios, was extremely poor as simulated by ESMs ($r = -0.11$).

3.5. Performance of ESM Model Families

Nine ESMs performed quite consistent in majority of biomes, while large discrepancies occurred in tropical savanna, tropical/subtropical grassland, temperate grassland, boreal broadleaf forest, subarctic grassland, subarctic arid shrubland/desert, tundra, and tidal marsh (Figure 6). For root and vegetation carbon density, the largest biases occurred in tidal marsh in the GFDL-ESM2M model, and the IPSL model family had moderate bias. Most models underestimated R/T ratios in majority of the biomes (Figure 6c). Specifically, all four model families overestimated R/T ratios in tropical/subtropical moist forest, and the CESM model family overestimated R/T ratios in boreal broadleaf forest, while the slight overestimations were observed by CESM and GFDL-ESM2M model families for tropical/subtropical dry forest, IPSL model family for temperate conifer forest, CESM, and GFDL-ESM2M and IPSL model families for temperate broadleaf forest (Figure 6c).

ESM performance varied substantially along the latitude (Figure 6). ESMs underestimated root carbon density in the Southern Hemisphere and tropical climate zones ($< -100\%$), while significantly overestimated in portions of the subarctic and arctic ($>200\%$ for the regions 50°N–70°N), and slight overestimation also occurred in a small area in the tropical zone (Figure 6a). Similar spatial patterns were detected in the simulation of total vegetation carbon (Figure 6b). Although the R/T ratios were simulated to be a relatively constant value across all ESMs (~0.2), the intermodel variation was dramatic in terms of comparing with observational data. NorESM model family had the largest discrepancy with observational data at the biome level, and IPSL model family had the largest discrepancy with observational data across latitudinal zones.

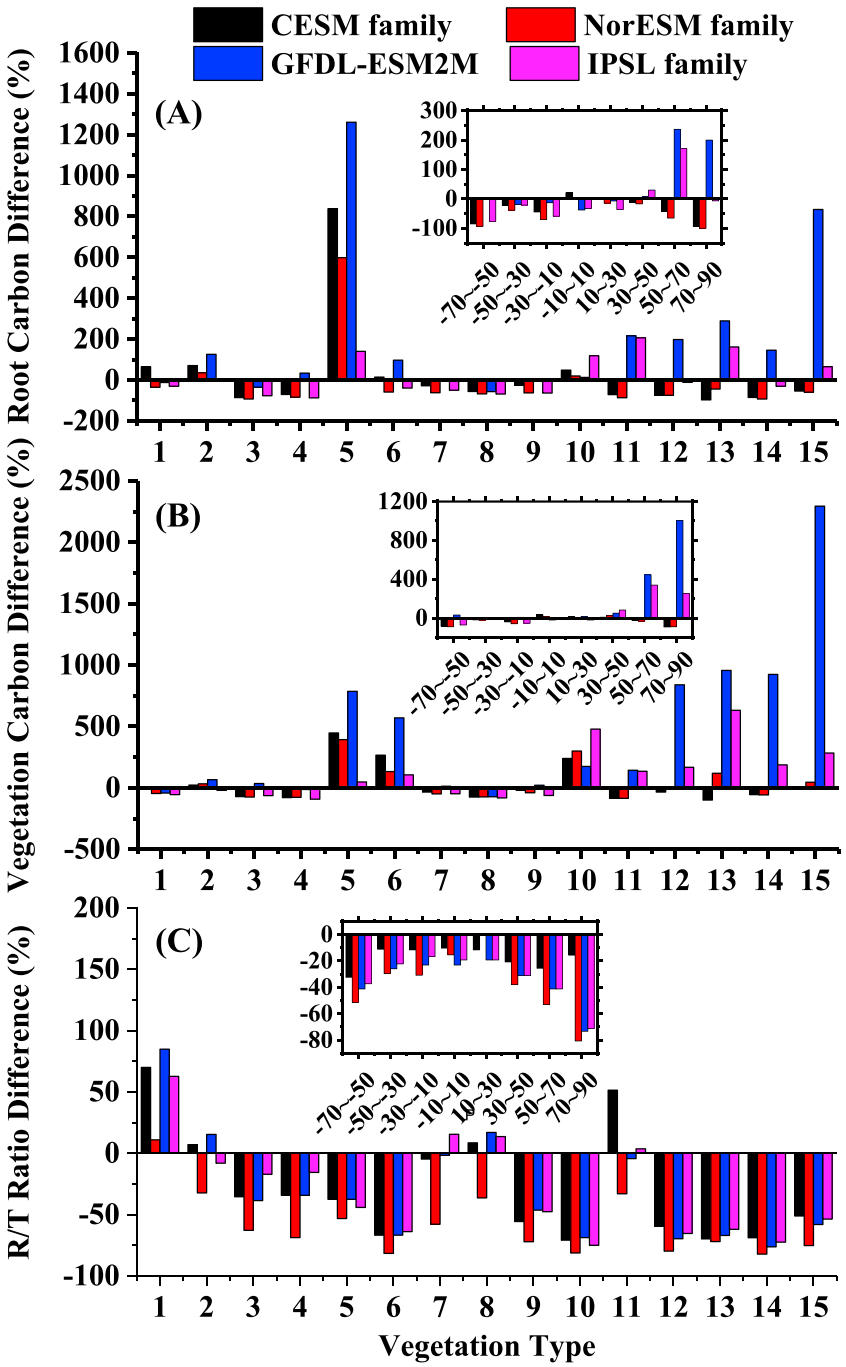

Figure 6. Differences between modeled root carbon density, vegetation carbon density (kg/m^2), and R/T ratios and observational data (ESMs mean minus observational data; positives indicate overestimation and negatives indicate underestimation; insets are the latitudinal comparison between modeled and observational results for root and vegetation densities and R/ratio; 1: tropical/subtropical moist forest; 2: tropical/subtropical dry forest; 3: tropical/subtropical moist woodland; 4: tropical/subtropical dry woodland; 5: tropical savanna; 6: tropical/subtropical grassland; 7: temperate conifer forest; 8: temperate broadleaf forest; 9: temperate shrubland; 10: temperate grassland; 11: boreal broadleaf forest; 12: subarctic grassland; 13: subarctic arid shrubland/desert; 14: tundra; 15: tidal marshes).

4. Discussion

4.1. Uncertainties in Carbon Densities as Simulated by ESMs

Our results showed that there were large discrepancies in ESM simulations of root and total vegetation carbon density. ESMs significantly underestimated root carbon and total vegetation carbon density in portions of the tropics but overestimated these important pools in the Arctic. Both the tropics and the Arctic are predicted to be highly sensitive to global climate changes [*Bonan*, 2008a, 2008b; *Pounds et al.*, 1999; *Overpeck et al.*, 1997], and the uncertainties in model estimation of carbon stocks in the tropics and the Arctic might significantly affect the projected carbon-climate feedbacks. Our results are consistent with other studies [*Friend et al.*, 2014; *Rammig et al.*, 2010], revealing large uncertainties in simulations of global carbon balance using ESMs, where these uncertainties were mainly attributed to the differences in the predicted change in the Amazonia tropical region [*Rammig et al.*, 2010] and the Arctic area [*Krinner et al.*, 2005; *Dunne et al.*, 2013].

The large discrepancies in carbon density between observations and ESM simulations were consistent across different scales. ESMs underestimated vegetation carbon density in the majority of tropical and temperate biomes but substantially overestimated vegetation carbon density in arctic biomes. The discrepancies of nine ESMs' simulation primarily occurred in three biomes: tidal marshes, temperate grassland, and tropical/subtropical grassland (Figure 3b).

4.2. Discrepancies in R/T Ratios as Simulated by ESMs

The underestimation of R/T ratios across all three climate zones suggested that either ESMs allocated less carbon belowground, or they simulated a faster root turnover rate. In tropical and temperate regions, the discrepancy in R/T between models and observations is likely due to less carbon allocation to belowground vegetation by the ESMs; in the arctic, the discrepancy is likely due to an overestimation of aboveground biomass by the ESMs. These large discrepancies suggest that the algorithm controlling carbon allocation are a key source of uncertainty [*Houghton*, 2007; *Arora et al.*, 2013; *Hoffman et al.*, 2014]. Furthermore, the relatively inflexible R/T ratios across ESMs (~0.2 across different biomes), which were significantly biased from the field observational data, may produce large uncertainties for carbon-climate feedback [*Friedlingstein et al.*, 2006]. A recent theoretical study [*Kleidon et al.*, 2007] demonstrated that the relatively narrow range of values for vegetation parameterization across different biomes in a coupled climate-vegetation model might have led to unrealistic multiple steady states when compared with a more variable representation of vegetation traits. It indicated that the estimation of vegetation carbon pools was not well represented, leading to an unrealistic carbon sink or source in land ecosystems [*Anav et al.*, 2010].

Total vegetation carbon is an important factor affecting carbon stocks in terrestrial ecosystems, and hence influencing how ecosystem carbon sequestrations respond to climate change [*Jackson et al.*, 1996; *Canadell et al.*, 1996; *Schenk and Jackson*, 2002; *Giardina et al.*, 2014]. In terrestrial ecosystems, vegetation carbon is eventually transferred to the soil through litter fall, root turnover, or death of individual plants, thus providing the substrate for the formation of soil organic carbon. Giardina et al. considered that warming-related increases in soil CO_2 efflux were explained by increased belowground carbon flux [*Giardina et al.*, 2014; *Bond-Lamberty and Thomson*, 2010]. Therefore, the underestimation of R/T ratios can significantly affect simulated soil carbon storage and belowground carbon fluxes [*Arora et al.*, 2013]. The relative importance of root carbon allocation for ecosystem carbon and nutrient fluxes, as well as long-term soil carbon storage, depends on the relative allocation of carbon to fine roots (micrometer to millimeter in diameter) compared with coarse roots (millimeter to centimeter in diameter). Fine roots are responsible for plant nutrient and water acquisition, and turnover on a timescale of month to years, while coarse roots and rhizomes are used for structure and storage, and for woody plants behave similarly to wood. The role of fine roots and their associated functional traits in land surface models and ESMs has been gradually gaining attention in recent years [*McCormack et al.*, 2015; *Warren et al.*, 2015]. Therefore, more field measurements on individual vegetation components will be critically important for better parameterizing and validating the allocation algorithm within land surface models.

Although CESM and NorESM share same land model (CLM), significantly different R/T ratios were simulated by CESM and NorESM. The CESM simulated R/T ratios were much closer to the observational data than those of the NorESM family. In addition, even though the land models use different carbon allocation mechanisms, they each represented a similar range of carbon ratios inside of the models (very close to 0.2).

4.3. Attributions of ESM Uncertainties

There are several potential reasons for the discrepancies we have shown between observed and modeled carbon density. First, vegetation parameters are not well constrained with field observations in tropical and the arctic regions. While data assimilation is currently becoming a popular technique to more properly combine numerical models with observational data [*Luo et al.*, 2012], we urgently need to explore and evaluate how current numerical implementations of vegetation allocation represent biological processes, particularly when we lack global-scale observations [*Thomas et al.*, 2015]. Second, ESMs are getting more and more complicated, and a growing number of mechanistic models require more field data to better constrain the processes incorporated in the model. For example, insufficient observational data in tropical and arctic regions and in biomes underlain by organic soils, such as tundra and tidal marshes, are a bottleneck for model parameterization [*Wullschleger et al.*, 2014]. Therefore, an integrative data-model fusion approach is highly needed to better evaluate the model outputs and improve model behavior.

Third, the mismatch between the vegetation maps used by ESMs and the real vegetation distribution should be acknowledged when interpreting this study. Vegetation classification is a critical factor determining the simulation accuracy of land surface models. If the land models do not represent the natural vegetation correctly, large simulation biases are likely [*Krinner et al.*, 2005; *Oleson et al.*, 2010; *Dunne et al.*, 2013]. In this study, the land surface model of LM3.0 only represents five vegetation types [*Dunne et al.*, 2013], while ORCHIDEE considers 12 vegetation types [*Krinner et al.*, 2005], and CLM4.0 classifies vegetation into 15 PFTs (plant functional types) [*Oleson et al.*, 2010]. Among these vegetation types, only CLM4.0 has an arctic PFT (a C3 arctic grass); LM3.0 and ORCHIDEE do not represent any specific vegetation type for the arctic region. Fourth, the temporal framework for data-model comparison might be another reason for the biases; model outputs were averaged for the time period of 1995–2005, while the field observational data span from 1980s to the 2000s and the exact date is often unavailable [*Gill and Jackson*, 2000; *Jackson et al.*, 1996].

Fifth, the vegetation carbon allocation algorithm varies among ESMs, though the small range of R/T ratios implemented in the ESMs we examined was far narrower than the observations [*Jackson et al.*, 1996; *Mokany et al.*, 2006], especially the two models of NorESM1-M and NorESM1-ME. The ESMs in this study represent three strategies for carbon allocation: fixed carbon ratios in CLM4.0 [*Thornton et al.*, 2009; *Yang et al.*, 2014], resource limitations theory in ORCHIDEE [*Parton et al.*, 1987], and dynamic phenology in LM3.0 [*Dunne et al.*, 2013] (Table 2). These strategies are inherent in the number of different carbon pools in the ESMs, with 20 carbon pools in CLM 4.0, 8 carbon pools in the ORCHIDEE, and 5 carbon pools in the LM 3.0. These carbon pools were linked to the physical functioning of the land surface in terms of solar radiation absorption, nutrient availability, and soil moisture dynamics. We note that the simulations of ESMs that employed more carbon pools were more consistent to the observations, especially in the arctic regions (Figure 6). To reflect the differences among model strategies, we have summarized the characteristics of the three models in the supplementary information (Table S2). We conclude that improvements are needed for ESM simulation of vegetation carbon allocation, consistent with *De Kauwe et al.* [2014].

Sixth, there were inconsistencies in data-model comparisons at the biome and climate zone levels, which were caused by the difference in data sets at these two scales. Biome-level data covered all biomes from different regions, while data for each climate zone represented an entire latitudinal band. Seventh, the comparisons between observational data and modeled output in this study were carried out at an annual scale, which ignored the seasonality of larger vegetation carbon density. This was necessary because the observational data compiled in this study was collected across multiple years, generally without any seasonal information. Also, the model output was annual vegetation carbon density according to the CMIP5 protocol. We acknowledged that this might have caused bias in our evaluation, and further comparison might be needed as data become available in near future and model output procedures change.

Last, but not least, the other modeling components in the ESMs might have contributed to the biases of simulated carbon density in root and total vegetation biomass. A recent study showed that the ESMs of CMIP5 were inadequate to represent ecosystem and climate feedback resulting from the arctic area [*Schaefer et al.*, 2011]. These discrepancies may be caused by difficulty in reproducing the climate conditions and the complex hydrological and thermal dynamics in ecosystems underlain by permafrost [*Walsh et al.*, 2002; *Schaefer et al.*, 2011], or by unoptimized parameters [*Schaefer et al.*, 2011]. In addition, the CESM and NorESM model families had similar performances regarding carbon density and R/T ratios, likely due to

the shared land surface model, CLM, in both ESMs. However, the magnitude of the model bias varied across biomes and along latitudes. For example, for most vegetation types including the tropical/subtropical moist forest, tropical/subtropical moist woodland, and tropical/subtropical grassland, vegetation carbon density simulated by the NorESM model family was about 20–150% less than that estimated by CESM model family (Figure 6).

5. Conclusions

We evaluated the carbon density in root and total vegetation biomass (and their ratio) as simulated by nine Earth system models used in CMIP5 against observational data; the comparisons were carried out across climate zones, biomes, along latitudinal gradients, and at the global scale. We identified large discrepancies between CMIP5 model results and observations in terms of their simulated carbon density and R/T ratios. ESMs significantly underestimated root carbon in parts of the tropical and temperate climate zones, but substantially overestimated total vegetation carbon density in the arctic climate zone. While R/T ratios are identified as an one important model parameter in simulating the carbon-climate feedback, nevertheless, our results showed that ESMs underestimated R/T ratios across most biomes (except the tropical moist forest) and at the global scale. In addition, the vegetation R/T ratios simulated by ESMs were relatively constant, averaging 0.2 across biomes and latitudes, which was significantly different from observed variation in R/T ratios in various biomes.

The large mismatch of ESMs in comparison to observational data underscores an urgent need to improve the carbon allocation algorithms within Earth system models. The functional dynamic allocation and optimization resource algorithms seemed to perform better for model simulation of carbon density and R/T ratios. However, intensive field campaigns that target an improved understanding of carbon allocations under complex of climatic and environmental conditions are still sorely needed to inform model structure and processes.

5.1. Author Contribution

X.S. and X.X designed the study. X.S., F.H., C.M.I., J.K., and X.X. contributed to data compilation and result interpretation. Y.Y. made contribution to the revision. X.S. and X.X wrote the manuscript with assistance from other coauthors.

5.2. Data Accessibility

The compiled site-level data are available as a supporting information. The global maps of root and total vegetation carbon density are available at the Carbon Dioxide Information Analysis Center [http://cdiac.ornl.gov], Oak Ridge National Laboratory, Oak Ridge, Tennessee. The model outputs from nine Earth system models were downloaded from the Earth System Grid-Center for Enabling Technologies, on the page http://pcmdi9.llnl.gov/.

Acknowledgments

The authors thank Yiqi Luo and Xiaochun Zhang for their comments on early version of this manuscript. We appreciated Aaron Ruesch and Holly K. Gibbs for sharing their global living biomass data for this study. Three anonymous reviewers had constructive comments that have significantly improved this manuscript. This study was supported through the Biogeochemistry Feedbacks Scientific Focus Area (BGC Feedbacks SFA), which is sponsored by the Regional and Global Climate Modeling (RGCM) Program in the Climate and Environmental Sciences Division (CESD) of the Biological and Environmental Research (BER) Program in the U.S. Department of Energy Office of Science. Support for X.S. and X.X. was proved by San Diego State University and the University of Texas at El Paso. Financial assistance was partially provided by the SPRUCE and NGEE Arctic projects, which are supported by the Office of Biological and Environmental Research in the U.S. Department of Energy Office of Science. Contributions by F.H., C.M.I., and J.K. were supported by the U.S. Department of Energy, Office of Science, Office of Biological and Environmental Research. Oak Ridge National Laboratory is managed by UT-Battelle, LLC, for the US Department of Energy under contract DE-AC05-00OR22725. Early work of this study was carried out at an internal cluster at the Climate Change Science Institute at Oak Ridge National Laboratory. This work partially used the Extreme Science and Engineering Discovery Environment (XSEDE), which is supported by National Science Foundation grant ACI-1053575. Authors state that there is no conflict of interest.

References

Anav, A., P. Friedlingstein, M. Kidston, L. Bopp, P. Ciais, P. Cox, C. Jones, M. Jung, R. Myneni, and Z. Zhu (2013), Evaluating the land and ocean components of the global carbon cycle in the CMIP5 Earth system models, *J. Clim.*, 6801–6843, doi: 10.1175/JCLI-D-12-00417.1.

Anav, A., F. D'Andrea, N. Viovy, and N. Vuichard (2010), A validation of heat and carbon fluxes from high-resolution land surface and regional models, *J. Geophys. Res.*, *115*, G04016, doi:10.1029/2009JG001178.

Arora, V. K., G. J. Boer, P. Friedlingstein, M. Eby, C. Jones, J. R. Christian, G. Bonan, L. Bopp, V. Brovkin, and P. Cadule (2013), Carbon–concentration and carbon–climate feedbacks in CMIP5 Earth system models, *J. Clim.*, *26*, 5289–5314.

Bonan, G. B. (2008a), Carbon cycle: Fertilizing change, *Nat. Geosci.*, *1*, 645–646.

Bonan, G. B. (2008b), Forests and climate change: Forcings, feedbacks, and the climate benefits of forests, *Science*, *320*, 1444–1449.

Bond-Lamberty, B., and T. Thomson (2010), Temperature-associated increases in the global soil respiration record, *Nature*, *464*, 579–581.

Cadule, P., P. Friedlingstein, L. Bopp, S. Sitch, C. Jones, P. Ciais, S. Piao, and P. Peylin (2010), Benchmarking coupled climate-carbon models against long-term atmospheric CO_2 measurements, *Global Biogeochem. Cycles*, *24*, GB2016, doi:10.1029/2009GB003556.

Canadell, J., R. Jackson, J. Ehleringer, H. Mooney, O. Sala, and E. D. Schulze (1996), Maximum rooting depth of vegetation types at the global scale, *Oecologia*, *108*, 583–595.

Carvalhais, N., M. Forkel, M. Khomik, J. Bellarby, M. Jung, M. Migliavacca, M. Mu, S. Saatchi, M. Santoro, and M. Thurner (2014), Global covariation of carbon turnover times with climate in terrestrial ecosystems, *Nature*, *514*, 213–217.

Chapin III, F. S., P. A. Matson, and P. M. Vitousek (2011), *Principles of Terrestrial Ecosystem Ecology*, pp. 123–156, Springer, New York.

De Kauwe, M. G., B. E. Medlyn, S. Zaehle, A. P. Walker, M. C. Dietze, Y. P. Wang, Y. Luo, A. Jain, B. Masri, and T. Hickler (2014), Where does the carbon go? A model–data intercomparison of vegetation carbon allocation and turnover processes at two temperate forest free-air CO_2 enrichment sites, *New Phytol.*, *203*, 883–899.

Dunne, J. P., J. G. John, E. Shevliakova, R. J. Stouffer, J. P. Krasting, S. L. Malyshev, P. Milly, L. T. Sentman, A. J. Adcroft, and W. Cooke (2013), GFDL's ESM2 global coupled climate–carbon Earth system models. Part II: Carbon system formulation and baseline simulation characteristics, *J. Clim.*, *26*, 2247–2267.

Flato, G. M. (2011), Earth system models: An overview, *Wiley Interdiscip. Rev. Clim. Change*, *2*, 783–800.

Friedlingstein, P., et al. (2006), Climate-carbon cycle feedback analysis: Results from the C4MIP model intercomparison, *J. Clim.*, *19*, 3337–3353.

Friend, A. D., et al. (2014), Carbon residence time dominates uncertainty in terrestrial vegetation responses to future climate and atmospheric CO_2, *Proc. Natl. Acad. Sci. U.S.A.*, *111*, 3280–3285.

Giardina, C. P., C. M. Litton, S. E. Crow, and G. Asner (2014), Warming-related increases in soil CO_2 efflux are explained by increased below-ground carbon flux, *Nat. Clim. Change*, *4*, 822–827.

Gill, R. A., and R. B. Jackson (2000), Global patterns of root turnover for terrestrial ecosystems, *New Phytol.*, *147*, 13–31.

Giorgetta, M. A., J. Jungclaus, C. H. Reick, S. Legutke, J. Bader, M. Böttinger, V. Brovkin, T. Crueger, M. Esch, and K. Fieg (2013), Climate and carbon cycle changes from 1850 to 2100 in MPI-ESM simulations for the Coupled Model Intercomparison project phase 5, *J. Adv. Model. Earth Syst.*, *5*, 572–597.

Good, P., J. M. Gregory, J. A. Lowe, and T. Andrews (2013), Abrupt CO_2 experiments as tools for predicting and understanding CMIP5 representative concentration pathway projections, *Clim. Dyn.*, *40*, 1041–1053.

He, Y., S. E. Trumbore, M. S. Torn, J. W. Harden, L. J. Vaughn, S. D. Allison, and J. T. Randerson (2016), Radiocarbon constraints imply reduced carbon uptake by soils during the 21st century, *Science*, *353*(6306), 1419–1424.

Hoffman, F. M., J. T. Randerson, V. K. Arora, O. Bao, P. Cadule, D. Ji, C. Jones, M. Kawamiya, S. Khatiwala, and K. Lindsay (2014), Causes and implications of persistent atmospheric carbon dioxide biases in Earth system models, *J. Geophys. Res. Biogeosci.*, *119*, 141–162, doi:10.1002/2013JG002381.

Houghton, R. A. (2007), Balancing the global carbon budget, *Annu. Rev. Earth Planet. Sci.*, *35*, 313–347.

IPCC (2003), *Good Practice Guidance for Land Use, Land-use Change and Forestry*, edited by J. M. Penman et al., chap. 3, Institute for Global Environmental Strategies (IGES) for the Intergovernmental Panel on Climate Change, Kanagawa, Japan.

Ise, T., C. Litton, C. Giardina, and A. Ito (2010), Comparison of modeling approaches for carbon partitioning: Impact on estimates of global net primary production and equilibrium biomass of woody vegetation from MODIS GPP, *J. Geophys. Res.*, *115*, G04025, doi:10.1029/2010JG001326.

Iversen, C. M., V. L. Sloan, P. F. Sullivan, E. S. Euskirchen, A. D. McGuire, R. J. Norby, A. P. Walker, J. M. Warren, and S. D. Wullschleger (2015), The unseen iceberg: Plant roots in arctic tundra, *New Phytol.*, *205*, 34–58.

Jackson, R. B., J. Canadell, J. R. Ehleringer, H. A. Mooney, O. E. Sala, and E. D. Schulze (1996), A global analysis of root distributions for terrestrial biomes, *Oecologia*, *108*, 389–411.

Jiang L., Y. Yan, O. Hararuk, N. Mikle, J. Xia, Z. Shi, J. Tjiputra, T. Wu, and Y. Luo (2015), Scale-dependent performance of CMIP5 Earth system models in simulating terrestrial vegetation carbon, *J. Clim.*, *28*(13), 5217–5232.

Jobbagy, E. G., and R. B. Jackson (2000), The vertical distribution of soil organic carbon and its relation to climate and vegetation, *Ecol. Appl.*, *10*, 423–436.

Jungclaus, J., S. Lorenz, C. Timmreck, C. Reick, V. Brovkin, K. Six, J. Segschneider, M. Giorgetta, T. Crowley, and J. Pongratz (2010), Climate and carbon-cycle variability over the last millennium, *Clim. Past*, *6*, 723–737.

Kleidon, A., K. Fraedrich, and C. Low (2007), Multiple steady-states in the terrestrial atmosphere-biosphere system: A result of a discrete vegetation classification?, *Biogeosciences*, *4*, 707–714.

Krinner, G., N. Viovy, N. de Noblet Ducoudré, J. Ogée, J. Polcher, P. Friedlingstein, P. Ciais, S. Sitch, and I. C. Prentice (2005), A dynamic global vegetation model for studies of the coupled atmosphere-biosphere system, *Global Biogeochem. Cycles*, *19*, GB1015, doi:10.1029/2003GB002199.

Luo, Y., et al. (2012), A framework of benchmarking land models, *Biogeosciences*, *9*, 3857–3874.

McCormack, M. L., E. Crisfield, B. Raczka, F. Schnekenburger, D. Eissenstat, and E. Smithwick (2015), Sensitivity of four ecological models to adjustments in fine root turnover rate, *Ecol. Modell.*, *297*, 107–117.

Mokany, K., R. Raison, and A. S. Prokushkin (2006), Critical analysis of root: Shoot ratios in terrestrial biomes, *Global Change Biol.*, *12*, 84–96.

Oleson, K. W., D. M. Lawrence, B. Gordon, M. G. Flanner, E. Kluzek, J. Peter, S. Levis, S. Swenson, E. Thornton, and J. Feddema (2010), Technical description of version 4.0 of the Community Land Model (CLM).

Overpeck, J., K. Hughen, D. Hardy, R. Bradley, R. Case, M. Douglas, B. Finney, K. Gajewski, G. Jacoby, and A. Jennings (1997), Arctic environmental change of the last four centuries, *Science*, *278*, 1251–1256.

Parton, W. J., D. S. Schimel, C. V. Cole, and D. S. Ojima (1987), Analysis of factors controlling soil organic matter levels in Great Plains grasslands, *Soil Sci. Soc. Am. J.*, *51*, 1173–1179.

Peng, S., P. Ciais, F. Chevallier, P. Peylin, P. Cadule, S. Sitch, S. Piao, A. Ahlström, C. Huntingford, and P. Levy (2015), Benchmarking the seasonal cycle of CO_2 fluxes simulated by terrestrial ecosystem models, *Global Biogeochem. Cycles*, *29*, 46–64, doi:10.1002/2014GB004931.

Pounds, J. A., M. P. Fogden, and J. H. Campbell (1999), Biological response to climate change on a tropical mountain, *Nature*, *398*, 611–615.

Raich, J. W., and W. H. Schlesinger (1992), The global carbon dioxide flux in soil respiration and its relationship to vegetation and climate, *Tellus B*, *44*, 81–99.

Rammig, A., T. Jupp, K. Thonicke, B. Tietjen, J. Heinke, S. Ostberg, W. Lucht, W. Cramer, and P. Cox (2010), Estimating the risk of Amazonian forest dieback, *New Phytol.*, *187*, 694–706.

Ruesch, A., and H. K. Gibbs (2008), New IPCC Tier-1 global biomass carbon map for the year 2000.

Schaefer, K., T. Zhang, L. Bruhwiler, and A. P. Barrett (2011), Amount and timing of permafrost carbon release in response to climate warming, *Tellus B*, *63*, 165–180.

Schenk, H. J., and R. B. Jackson (2002), Rooting depths, lateral root spreads and belowground/aboveground allometries of plants in water-limited ecosystems, *J. Ecol.*, *90*, 480–494.

Schuur, E. A. G., A. D. McGuire, C. Schädel, G. Grosse, J. W. Harden, D. J. Hayes, G. Hugelius, C. Koven, P. Kuhry, and D. Lawrence (2015), Climate change and the permafrost carbon feedback, *Nature*, *520*, 171–179.

Stephenson, N. L., and P. J. Mantgem (2005), Forest turnover rates follow global and regional patterns of productivity, *Ecol. Lett.*, *8*, 524–531.

Taylor, K. E., V. Balaji, S. Hankin, M. Juckes, B. Lawrence, and S. Pascoe (2011), CMIP5 data reference syntax (DRS) and controlled vocabularies. [Available at http://cmip-pcmdi.llnl.gov/cmip5/docs/cmip5_data_reference_syntax.pdf.]

Thomas, R. Q., E. Brookshire, and S. Gerber (2015), Nitrogen limitation on land: How can it occur in Earth system models?, *Global Change Biol.*, *21*, 1777–1793.

Thornton, P. E., S. Doney, K. Lindsay, J. K. Moore, N. M. Mahowald, J. T. Randerson, I. Y. Fung, J. F. Lamarque, J. Feddema, and Y. H. Lee (2009), Carbon-nitrogen interactions regulate climate-carbon cycle feedbacks: Results from an atmosphere-ocean general circulation model, *Biogeosciences*, *6*, 2099–2120.

Todd-Brown, K., J. Randerson, F. Hopkins, V. Arora, T. Hajima, C. Jones, E. Shevliakova, J. Tjiputra, E. Volodin, and T. Wu (2014), Changes in soil organic carbon storage predicted by Earth system models during the 21st century, *Biogeosciences*, *11*, 2341–2356.

Todd-Brown, K., J. Randerson, W. Post, F. Hoffman, C. Tarnocai, E. Schuur, and S. Allison (2013), Causes of variation in soil carbon simulations from CMIP5 Earth system models and comparison with observations, *Biogeosciences*, *10*, 1717–1736.

Walsh, J. E., V. M. Kattsov, W. L. Chapman, V. Govorkova, and T. Pavlova (2002), Comparison of Arctic climate simulations by uncoupled and coupled global models, *J. Clim.*, *15*, 1429–1446.

Warren, J. M., P. J. Hanson, C. M. Iversen, J. Kumar, A. P. Walker, and S. D. Wullschleger (2015), Root structural and functional dynamics in terrestrial biosphere models–evaluation and recommendations, *New Phytol.*, *205*, 59–78.

Weng, E., and Y. Luo (2011), Relative information contributions of model vs. data to short-and long-term forecasts of forest carbon dynamics, *Ecol. Appl.*, *21*, 1490–1505.

Wullschleger, S. D., H. E. Epstein, E. O. Box, E. S. Euskirchen, S. Goswami, C. M. Iversen, J. Kattge, R. J. Norby, P. M. van Bodegom, and X. Xu (2014), Plant functional types in Earth system models: Past experiences and future directions for application of dynamic vegetation models in high-latitude ecosystems, *Ann. Bot.*, *114*(1), 1–16, doi: 10.1093/aob/mcu077.

Xu, X., P. E. Thornton, and W. M. Post (2013), A global analysis of soil microbial biomass carbon, nitrogen and phosphorus in terrestrial ecosystems, *Glob. Ecol. Biogeogr.*, *22*, 737–749.

Xu, X., J. P. Schimel, P. Thornton, X. Song, F. Yuan, and S. Goswami (2014), Substrate and environmental controls on microbial assimilation of soil organic carbon: A framework for Earth system models, *Ecol. Lett.*, *17*, 547–555.

Xu, X., J. P. Schimel, I. A. Janssens, X. Song, C. Song, G. Yu, R. L. Sinsabaugh, D. Tang, X. Zhang, and P. E. Thornton (2017), Global pattern and controls of soil microbial metabolic quotient, *Ecol. Monogr.*, doi: 10.1002/ecm.1258.

Yang, X., P. E. Thornton, D. M. Ricciuto, and W. M. Post (2014), The role of phosphorus dynamics in tropical forests—A modeling study using CLM-CNP, *Biogeosciences*, *11*, 1667–1681.